UNIVERSITY OF LEEDS

This is a repository copy of *Fresh and hardened state properties of hybrid graphene oxide/nanosilica cement composites*.

White Rose Research Online URL for this paper:
http://eprints.whiterose.ac.uk/147585/

Version: Accepted Version

Article:
Newell, M and Garcia-Taengua, E orcid.org/0000-0003-2847-5932 (2019) Fresh and hardened state properties of hybrid graphene oxide/nanosilica cement composites. Construction and Building Materials, 221. pp. 433-442. ISSN 0950-0618

https://doi.org/10.1016/j.conbuildmat.2019.06.066

(c) 2019, Elsevier Ltd. This manuscript version is made available under the CC BY-NC-ND 4.0 license https://creativecommons.org/licenses/by-nc-nd/4.0/

Reuse
This article is distributed under the terms of the Creative Commons Attribution-NonCommercial-NoDerivs (CC BY-NC-ND) licence. This licence only allows you to download this work and share it with others as long as you credit the authors, but you can't change the article in any way or use it commercially. More information and the full terms of the licence here: https://creativecommons.org/licenses/

Takedown
If you consider content in White Rose Research Online to be in breach of UK law, please notify us by emailing eprints@whiterose.ac.uk including the URL of the record and the reason for the withdrawal request.

eprints@whiterose.ac.uk
https://eprints.whiterose.ac.uk/

Fresh and hardened state properties of hybrid graphene oxide/nanosilica cement composites

Michael Newell [1], and Emilio Garcia-Taengua [2,*]

[1] Gawn Associates, Cambridge CB24 3DQ, United Kingdom; mike@gawnassociates.com

[2] School of Civil Engineering, University of Leeds, Leeds LS2 9JT, United Kingdom; E.Garcia-Taengua@leeds.ac.uk

***** Correspondence: E.Garcia-Taengua@leeds.ac.uk; Tel.: +44-(0)1133430698

Abstract: This study looks into the combined effects of nanosilica (NS) and graphene oxide (GO) when jointly added to cement-based systems and their interaction with superplasticizers (SP). Cement pastes with NS and GO contents of up to 3% and 0.03% over cement weight respectively, and with superplasticizer dosages varying between 0.6% and 1.2%, were analyzed by means of the Marsh cone, calorimetry, uniaxial compression and water sorptivity tests. Results showed significant improvements resulting from the combined addition of NS and GO, and that their efficiency was significantly improved by increasing the SP dosage. Optimal GO and NS contents were found to be 0.018% and 2.2% respectively.

Keywords: cement; graphene; nanosilica; rheology; strength; sorptivity.

1. INTRODUCTION

The growing demand for special concretes or high-performance cement-based materials, which typically include significant amount of powders other than cement, together with the continued technological advancements facilitating the design and manipulation of materials at the nanoscale have made the use of nanomaterials as low-dosage cement additions increasingly attractive to researchers and industry [1,2]. Amongst them, the most studied are nanosilica, nano-iron oxide, nano-alumina, or nano-titanium oxide [3–5]. More recently, the possibilities of graphene-based materials in cement-based systems have also attracted attention [6,7]. This new suite of potential constituents of cement-based materials adds new possibilities as they can be used not only in combination with cement but also with binary or ternary cement blends that incorporate supplementary cementitious materials such as fly ash (FA), silica fume (SF), slags or mineral fillers [8,9].

Although in different degrees, the addition of nanoparticles has been reported to improve the mechanical properties of hardened cement-based materials, which in turn affects transport properties relevant to durability [10], as a consequence of their effect on the development of cement hydration reactions. This is achieved through three main mechanisms [9,11]: pozzolanic activity, filler effect, and by providing additional nucleation sites for the cement hydration products. Their small particle size and high specific surface area are determining factors to these mechanisms, but at the same time increase water demand and alter the rheology of fresh mixes, which generally leads to decreased workability [3,12]. This, together with their tendency to agglomerate, can result in the nanoparticles being poorly dispersed and not fully realizing their potential [13,14].

Nanosilica (NS), in addition to the small particle size and high specific surface area, has a high content in amorphous silica and outperforms silica fume in terms of pozzolanic activity [8], however its effect on cement hydration is mostly due to the increase in

nucleation sites and its filler effect [9,11,15]. When the NS is added at rates between 0.75% and 0.9% over cement weight, increases in compressive strength between 12% and 24.4% at 28 days have been reported [16,17]. Higher increases, of up to 70%, have been reported for NS dosages up to 4% [18]. However, the factor of improvement decreases beyond that point, which has been attributed to poor dispersion and agglomeration problems [17,19,20]. Garcia-Taengua, et al. [9] observed an optimum NS dosage to maximize compressive strength at 1.63%, and confirmed that increasing the dosage of superplasticizer (SP) is associated with higher compressive strength values and accelerated cement hydration, which confirms that the use of SP is effective in minimizing the agglomeration of NS particles in fresh cement systems [9].

Graphene oxide (GO) is an oxidized form of graphene and has high specific surface area. Its production consists in the oxidization of graphite using strong oxidizing agents, followed by the exfoliation of the resulting graphite oxide [3,21,22]. The oxidization gives it hydrophilic properties, enhancing its dispersability in water due to oxygen-containing functional groups [21,23].

The addition of GO in doses between 0.03% and 0.05% over cement weight has been reported to increase compressive strength in up to 47% [6,24–27], due to its accelerating effect on the dissolution rate of cement by providing additional nucleation sites, enhancing the formation of cement hydration products [23,27,28]. The introduction of GO also refines the pore structure of the cementitious matrix, and some studies report optimal GO doses around 0.02% over the weight of cement [28]. Reductions in the water sorptivity of up to 44% have been observed in cement pastes with GO contents between 0.02% and 0.04% over cement weight [27,29]. However, the incorporation of GO, especially at relatively high dosages, has been found to cause significant reductions in workability. Cement pastes with GO contents between 0.05% and 0.08% over cement weight have been

reported to have 36% to 50% less workability than their cement-only counterparts [9,24,30].

A number of studies have explored the possibilities of incorporating more than one type of nanoparticle to cement-based pastes or mortars, sometimes in combination with mineral additions [5,31]. The interest in such systems is motivated by the possibility that the complex interactions between different constituents result in synergies that can modify the mechanical properties or the workability of fresh mixes. Also, the addition of two nanomaterials allows a higher total content to be added while maintaining the relative content of each below their maxima for optimal performance.

To date, there are very few published studies concerning the effect of NS and GO on fresh and hardened state properties of cement-based materials when both are used together [32-33]. This study aimed at assessing the effect of different relative amounts of NS and GO on the workability, cement hydration, compressive strength and water sorptivity, and how the SP dosage affected the interaction between NS, GO, and cement. A number of pastes were produced and tested, and multiple linear regression was applied to fit predictive equations to the experimental results. These equations were used to plot contour plots for the different properties under study in order to assess the relative impact of NS and GO contents and SP dosage.

2. MATERIALS AND METHODS

A total of 18 different cementitious pastes with a constant water-to-binder ratio of 0.40 were produced, replacing part of the cement by NS and GO at three different levels: 0%, 1% and 3% for the NS, and 0.01% and 0.03% for the GO, percentages referred to the total binder weight. These values were selected to cover a sufficiently wide range and include the contents most commonly referred to in literature. The SP dosage was considered at two

levels: 0.6% and 1.2% over the weight of cement. These dosages corresponded to 0.75 and 1.25 times the average dose recommended by the manufacturer, and were selected to ensure that the SP was dosed within its effective range. The Marsh cone test was used to measure the flowability of the fresh mixes, and heat of hydration curves were obtained for all combinations by means of calorimetry tests. Compressive strength and water sorptivity were measured at the age of 28 days.

2.1. Materials

The materials used were: distilled water, cement, NS, GO, and SP. Portland cement type CEM I 52.5N conforming to EN 197-1:2000 was used. The NS was Cembinder® 22 produced by AkzoNobel, an aqueous dispersion of colloidal silica containing 40% of solids by weight, with an average particle size of 12 nm and a specific surface area of 220 m^2/g. The GO consisted of highly oxidized monolayer graphene sheets with a lateral dimension of less than 4 microns, predispersed in water at a concentration of 5 mg/mL, and produced by 2-DTech Versarien®. The chemical composition of the cement, NS, and GO is given in Table 1. The superplasticizer used was a commercially available polycarboxylic ether based high range water reducer, with a solid content of 40% and a specific gravity of 1.09.

Table 1. Equivalent oxides composition of the cement and NS used (mass percentage).

	SiO_2	Al_2O_3	Fe_2O_3	MgO	CaO	Na_2O	K_2O	SO_3	P_2O_5	L.O.I.
Cement	21.01	4.92	2.84	2.20	64.52	0.20	0.71	2.53	0.11	1.26
NS	99.40	0.08	-	-	-	0.45	-	-	-	-

Table 2. Elemental composition of the GO used (values in mass percentage).

	C	H	N	S	O
GO	55-65	0-1	0-1	0-2	30-40

2.2. Preparation of Cement Pastes

For each of the 18 mixes, two batches were prepared. The first batch of 1.5 L was used for the Marsh cone test and to cast 4 50-mm cubic specimens. A second, smaller batch of 4 mL was used for the calorimetry test. Water was premixed with the corresponding amounts of NS, GO, and SP for 60 seconds, to ensure adequate dispersion of the nanoparticles, and then the corresponding amount of cement was added to the mix. The mixing was carried out in a planar-action high-shear mixer for 7 minutes. The same mixing regime was followed for all mixes, starting at a constant speed of 140 rpm for 4 minutes. At that point, the mixer was stopped for 1.5 minutes and a spatula was used to remix the material that adhered to the mixer surfaces, after which the mixing was resumed for 1.5 minutes.

2.3. Marsh Cone Test

Immediately after mixing, the flowability of the pastes was measured by means of the Marsh cone test. The dimensions of the Marsh cone used were compliant with the standard EN 445:2007 [34], and the inner surface was always pre-wetted to minimize the friction with the fresh material. The cone was filled with a total volume of 750 mL of fresh cement paste, and the time it took for 700 mL of mix volume to flow out of the cone, t_{700} in seconds, was measured.

2.4. Calorimetry Test

Isothermal calorimetry tests were performed using a TAM air calorimeter set at a constant temperature of 21ºC. The heat of hydration was measured and recorded for a period of at least 5 days. As a result, heat of hydration curves were obtained, showing the evolution of the heat rate in mW/g against time. From each curve, the values of four representative parameters were retained for the quantitative analysis:

- The maximum heat rate or peak of hydration q_{max}, in mW/g, which informed of the maximum intensity of cement hydration reactions.
- The minimum heat rate q_{min}, in mW/g, which informed of the lowest intensity of cement hydration reactions during the dormant period.
- The times to the maximum and minimum heat rates, $t(q_{max})$ and $t(q_{min})$ respectively, measured in hours, to assess the acceleration or deceleration of cement hydration.

These parameters have proven useful in the analysis of cement hydration kinetics and their relationship with the mechanical properties of hardened pastes or mortars [9]. A graphical definition is shown in Figure 1 for illustration purposes.

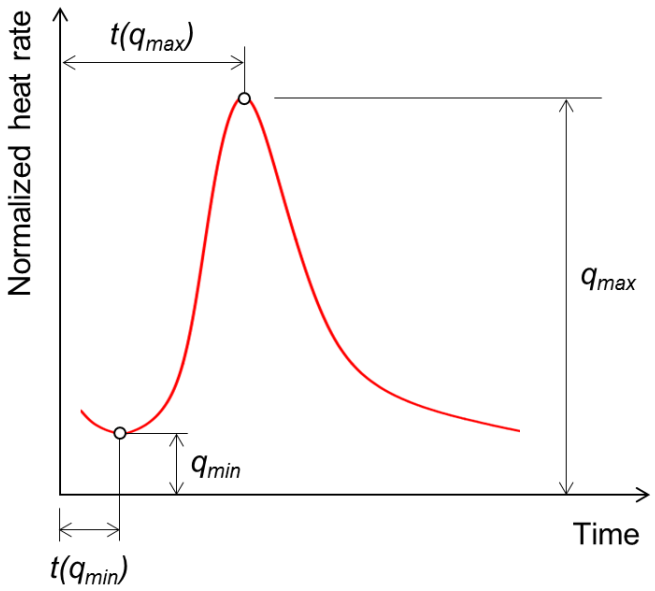

Figure 1. Definition of quantitative parameters from the calorimetry tests, based on [9].

2.5. Casting and Curing of Specimens

From each mix, four 50 mm-side cubic specimens were produced for the compression and water sorptivity tests. Immediately after casting, specimens were vibrated for 15 seconds to ensure adequate compaction of the fresh material. The specimens were stored for 24 hours before demolding. The molds used were compliant with EN 196-1:1995 [35], allowing easy demolding and manipulation without damaging the exposed surfaces, which was

159 especially important in the specimens to be used for the water sorptivity tests. After
160 demolding, all specimens were kept in controlled conditions, at a temperature of 20°C and
161 99% relative humidity, until they reached the 28 days of age.
162
163 **2.6. Uniaxial Compression Test**
164 At the age of 28 days, cubic specimens were tested in uniaxial compression to EN 12390-
165 3:2009 [36]. The load was applied at a constant rate of 55 kN/min, and the maximum load
166 value to the nearest 0.2 kN was recorded to determine the compressive strength, in MPa.
167 For each set of specimens from the same mix, the average compressive strength, f_c, and the
168 standard deviation, $s(f_c)$, both expressed in MPa, were obtained.
169
170 **2.7. Water Sorptivity Test**
171 The water sorptivity test was carried out to ASTM C1585-13 [37]. In order to determine
172 their dry mass, the cubes to be tested for water sorptivity were oven-dried to constant mass
173 at a temperature of 50ºC. Then they were exposed to water on a single 50x50mm face,
174 keeping the water level at a constant level throughout the test, approximately 5mm above
175 the base of the specimen. Measurements of the wet mass of each sample were taken at the
176 times of 1, 4, 9, 16, 25, 36, 49 and 64 minutes into the test. The water sorptivity
177 coefficient, k, expressed in $cm/s^{0.5}$, was determined as follows:
178

$$k = \frac{(M(t) - M_0)/\rho}{A\sqrt{t}} \quad (1)$$

179
180 where t is time (seconds); M(t) is the wet mass (grams); M_0 is the dry mass (grams); ρ is
181 the density of water (1 g/cm^3), and A is the area of the surface exposed to water, 25 cm^2.
182

3. RESULTS AND DISCUSSION

3.1. Fresh State Performance: Flowability

The flow times obtained from the Marsh cone test, t_{700}, expressed in seconds, are shown in Table 3. The relationship between this parameter and the dosages of NS, GO and SP was modelled by means of multiple linear regression analysis. The fitted equation was used to produce contour plots of t_{700} with respect to NS, GO, and SP dosages, thus allowing for a clear interpretation of the experimental results.

Table 3. Marsh cone test results.

SP (%)	GO (%)	NS (%)	t_{700} (s)
0.6	0.00	0	15.3
1.2	0.00	0	20.3
0.6	0.00	1	28.6
1.2	0.00	1	21.1
0.6	0.00	3	-
1.2	0.00	3	-
0.6	0.01	0	15.5
1.2	0.01	0	17.0
0.6	0.01	1	37.9
1.2	0.01	1	19.1
0.6	0.01	3	-
1.2	0.01	3	-
0.6	0.03	0	27.5
1.2	0.03	0	29.6
0.6	0.03	1	62.0
1.2	0.03	1	29.9
0.6	0.03	3	-
1.2	0.03	3	-

For some of the mixes, t_{700} was not defined because the paste was too thick and did not flow through the Marsh cone, and in consequence it was decided to consider the inverse $1/t_{700}$, expressed in seconds^{-1}, as the response parameter for the regression analysis. Using

this transformation, t_{700} was approximated to infinity in those cases where the paste was too thick to flow, making $1/t_{700}$ equal to zero, therefore having all cases described quantitatively. As a result, the regression analysis to correlate the Marsh cone test measurements to the relative amounts of NS, GO, and SP, could be performed without bias. The predictive equation obtained was very accurate (R-squared=0.95), where t_{700} times are expressed in seconds, and NS, GO, and SP dosages are expressed as percentage of the total binder weight:

$$\frac{1}{t_{700}} = (62.5 + (13.5 - 15.5\,SP)NS^2 + (46.4SP - 61.3)NS + (277.3NS - 836.4)GO) \times 10^{-3} \quad (2)$$

Figure 2 shows the t_{700} flow times as modelled by equation (2) against the relative amounts of NS and GO, for the two SP dosages considered in this study. It can be observed that, in general, higher GO contents led to higher t_{700} values and therefore less flowable mixes. The same can be said in relation to NS, which had a more pronounced effect on the reduction of workability, yielding even mixes too thick to flow.

In the absence of NS, the effect of increasing GO contents on the flowability of the mixes is not sensitive to variations the SP dosage. The addition of GO at 0.03% increases the average flow time from 16 to 27 seconds, which represents an increase of 70.3%. However, the relative increase of flow times caused by the addition of GO is lower when NS is also present in the mix. For instance, when SP is dosed at 1.2% and NS is incorporated at 1.5%, the addition of GO at 0.03% yields an average increase of 42% in t_{700} values, and this percentage is reduced to 39% if NS is dosed at 2%. These values are consistent with the results of previous studies, which have reported reductions in workability of up to 42% for GO dosages up to 0.05% [6]. However, when both NS and GO are present in the mix, it is NS that dominates the reduction in flowability, which has

been attributed to the generally finer particle size of NS and the fact that it is incorporated in volumes much higher than GO [3].

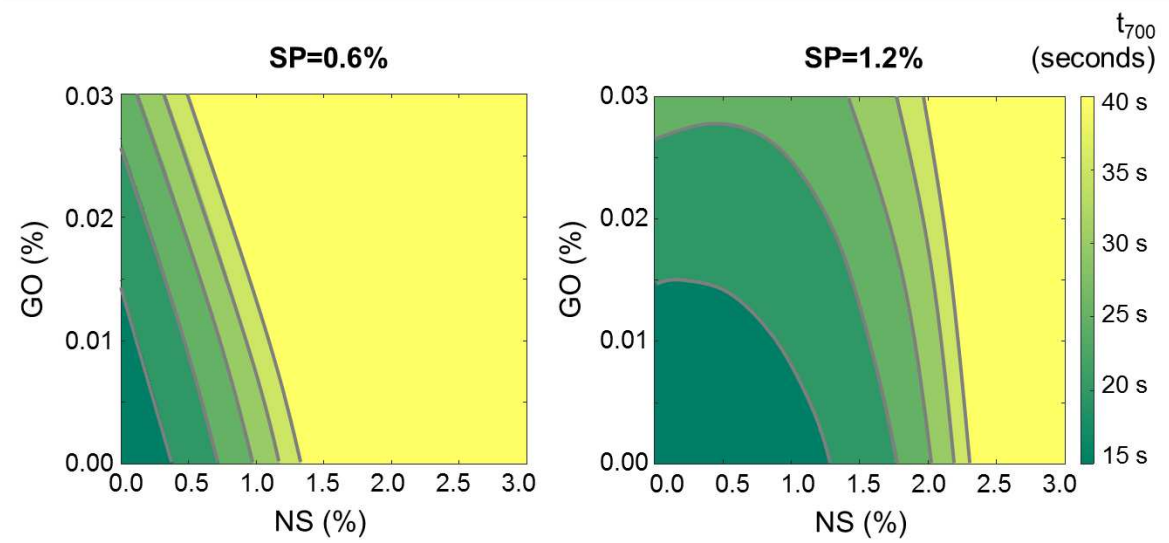

Figure 2. Flow time vs GO and NS contents, for two different SP dosages.

Although equation (2) can produce estimated t_{700} values up to infinity, predicted t_{700} values higher than 40 seconds generally correspond to mixes that do not flow through the Marsh cone. As a result, the intersection of the response surfaces with the horizontal plane t_{700} = 40 seconds can be used to identify the maximum NS content that can be incorporated to a mix without making it unflowable. As Figure 2 shows, this maximum NS content varies with the GO content as well as the SP dosage. If the SP dosage is 1.2%, the maximum NS content is 2.3% in the absence of GO, or 2% if GO is present at 0.03%. However, if the SP dosage is reduced from 1.2% to 0.6%, the maximum NS contents are significantly decreased: 1.3% in the absence of GO, or 0.5% if the GO is present at 0.03%. This confirms that, although GO and NS both have an impact on flowability, when they are dosed within the ranges considered in this study it is the amount of NS which can become the determining factor, and its effect on flowability is markedly affected by the SP dosage.

The effect of SP dosage and its interaction with NS and GO contents is more clearly seen in Figure 3, which plots equation (2) with respect to GO content and SP dosage, for three different NS contents.

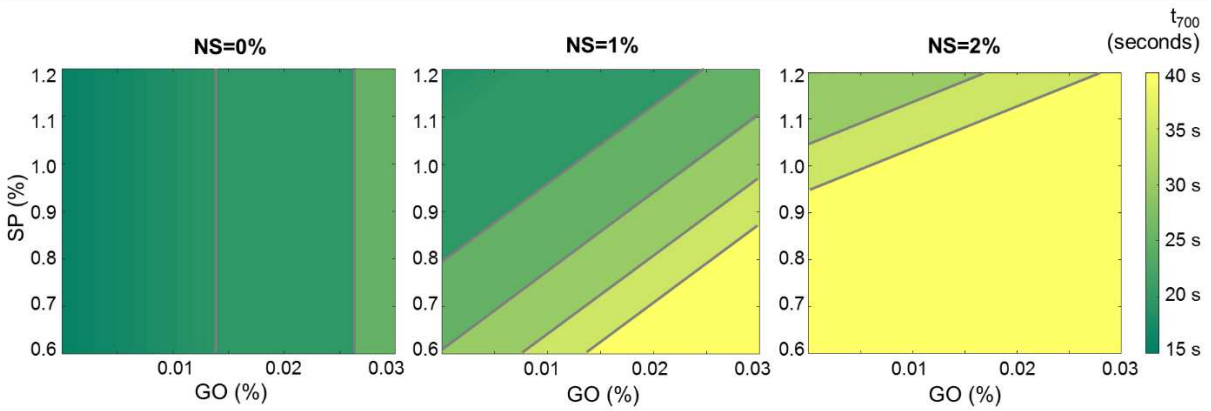

Figure 3. Flow time vs GO content and SP dosage, for three different NS contents.

Increasing the SP dosage within the range recommended by the manufacturer had little to no effect on the flowability of the mixes without NS, but became more significant with the addition of NS. When the NS content was 1%, increasing the SP dosage from 0.6% to 1.2% led to significant reductions in t_{700} values: between 40% and 59%, for GO contents of 0% and 0.03% respectively. Dosing the SP at 0.6% was in general sufficient for mixes with NS contents lower than 1% and GO contents not higher than 0.02%. However, for NS contents higher than 1%, adequate flowability required SP dosages beyond 0.6%, and mixes with an NS content of 2% required SP dosages of at least 1%. On the other hand, the effect of increasing GO contents on the minimum SP dosage required for good flowability was comparatively minor: the use of GO at 0.03% increased the required SP dosage but only from 1% to 1.2% when the NS content was 2%. In summary, from Figures 2 and 3 it can be concluded that, although the addition of NS and GO is generally detrimental to flowability and needs to be counterbalanced by increasing the SP dosage, the impact of NS on flowability is significantly higher than that of GO. In other words: in terms of the minimum SP requirements to maintain flowability, the introduction of NS in dosages of up

to 3% is clearly more demanding than the introduction of GO in dosages of up to 0.03%, which indicates that, within those dosage ranges, dispersion is less of a problem with GO than with NS.

3.2. Calorimetry Test Results

The results obtained from the calorimetry tests are shown in Table 4. Multiple linear regression was used to correlate each of these four parameters to the dosages of NS, GO and SP, all expressed in percentage.

Table 4. Calorimetry test results: quantitative parameters.

SP (%)	GO (%)	NS (%)	q_{max} (mW/g)	$t(q_{max})$ (h)	q_{min} (mW/g)	$t(q_{min})$ (h)
0.6	0.00	0.0	1.689	21	0.256	8
0.6	0.00	1.0	1.710	13	0.441	4
0.6	0.00	3.0	1.809	10	0.513	3
0.6	0.01	0.0	1.772	18	0.247	6
0.6	0.01	1.0	1.882	11	0.411	2
0.6	0.01	3.0	2.055	9	0.566	2
0.6	0.03	0.0	1.880	19	0.286	7
0.6	0.03	1.0	1.997	11	0.463	3
0.6	0.03	3.0	1.998	10	0.526	2
1.2	0.00	0.0	1.542	30	0.235	10
1.2	0.00	1.0	1.905	19	0.335	5
1.2	0.00	3.0	1.971	13	0.483	4
1.2	0.01	0.0	1.702	29	0.247	10
1.2	0.01	1.0	2.173	17	0.352	5
1.2	0.01	3.0	2.055	12	0.445	3
1.2	0.03	0.0	1.771	30	0.244	10
1.2	0.03	1.0	1.718	19	0.306	5
1.2	0.03	3.0	1.904	12	0.488	3

The equations obtained, which accurately fitted the experimental results (R-squared values ranging between 0.75 and 0.98) are the following:

$$t(q_{max}) = 10.42 - 8.07NS + 2.43NS^2 - 220.8GO + 6250GO^2 + SP(16.51 - 4.19NS) \quad (3)$$

$$q_{max} = 1.65 + 534GO^2 + SP(22.4GO - 1221GO^2 + 0.24NS - 0.052NS^2) \quad (4)$$

$$t(q_{min}) = 4.47 + SP(4.72 - 1.25NS) - 125GO + 3333GO^2 - 4.44NS + 1.24NS^2 \quad (5)$$

$$q_{min} = 0.35 - 0.11SP + 0.16NS - 0.024NS^2 \quad (6)$$

Figure 4 shows the contour plots for $t(q_{max})$, as per equation (3), corresponding to the SP dosages of 0.6% and 1.2%. The introduction of NS clearly accelerated cement hydration, and increasing NS contents were associated with significantly reduced $t(q_{max})$ times. The accelerating effect of NS was maximized when present in contents in the region of 2% to 2.5%, which led to reductions in $t(q_{max})$ between 55% and 60%, for SP dosages between 0.6% and 1.2% respectively. On the other hand, the GO content that minimized $t(q_{max})$ was 0.018%, but in comparison the effect of GO turned out to be much more modest than that of NS. In the absence of NS, the addition of GO at 0.018% caused $t(q_{max})$ values to decrease by 8% in average. For NS contents in the region of 2%, the slightly accelerating effect of GO on cement hydration gained relative significance, and its addition at 0.018% yielded reductions in $t(q_{max})$ between 16% and 21%, for SP dosages of 1.2% and 0.6% respectively. Therefore, the accelerating effect of GO is most capitalized when added in combination with NS.

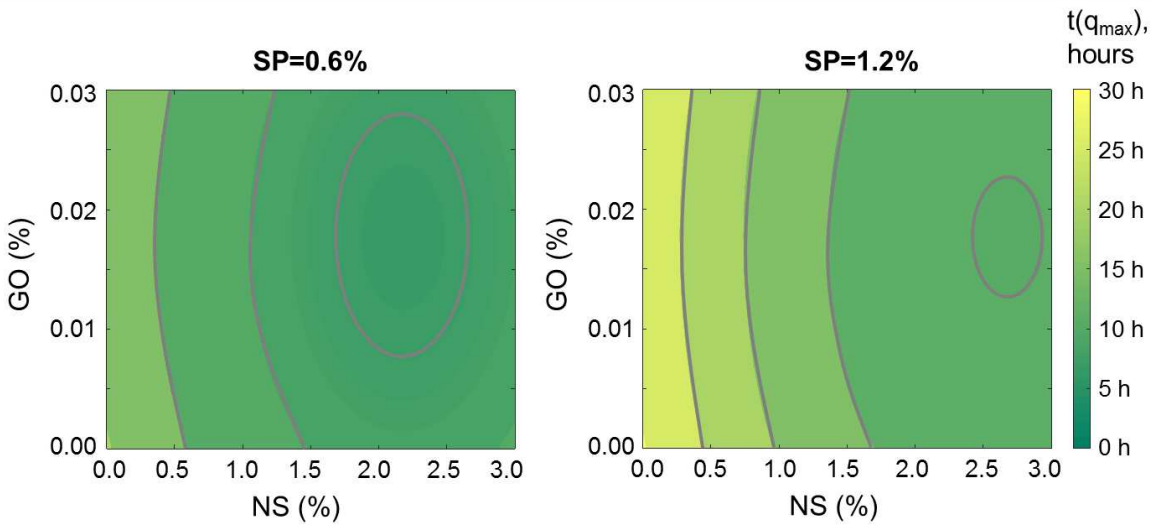

Figure 4. Time to the peak of hydration vs NS and GO contents, for two SP dosages.

The interaction between the SP dosage and the NS content proved statistically significant and this is reflected in equation (3), where the coefficient multiplying SP is a function of NS content. Figure 5 plots equation (3) with respect to NS content and SP dosage, assuming a GO content of 0.018%. Increasing the SP dosage had a retarding effect on cement hydration, generally increasing $t(q_{max})$ values, which is consistent with previous literature [38]. However, the magnitude of this increase was strongly dependent on the NS content. Whilst increasing the SP dosage from 0.6% to 1.2% delayed the peak of hydration by 10 hours in average in the absence of NS, this delay was reduced to 3.7 hours or 2.1 hours when NS contents of 2.4% or 3%, respectively, were considered. In consequence, these findings point out that increasing the SP dosage when the NS content is increased is critical not only to workability but also to hydration kinetics.

In fact, increasing the SP dosage was found to have a positive impact on the intensity of the peak of hydration, q_{max}, when NS and GO are present in the mix. Figure 6 shows equation (4) plotted against NS content and SP dosage assuming the GO content as 0.018%, and it can be seen that the effect of adding NS at 2.4% on q_{max} was clearly enhanced by increasing the SP dosage. The addition of NS at 2.4% combined with

increasing the SP dosage to 1.2% increased q_{max} in up to 21.4% for GO contents in the region of 0.018%. This positive synergy between NS and SP confirmed that increasing the SP dosage improves the efficiency of NS particles when used together with GO, which has also been observed in cementitious systems with NS and FA [9], and has been linked to the SP contribution to enhancing the dispersion of NS particles in the fresh mix [13].

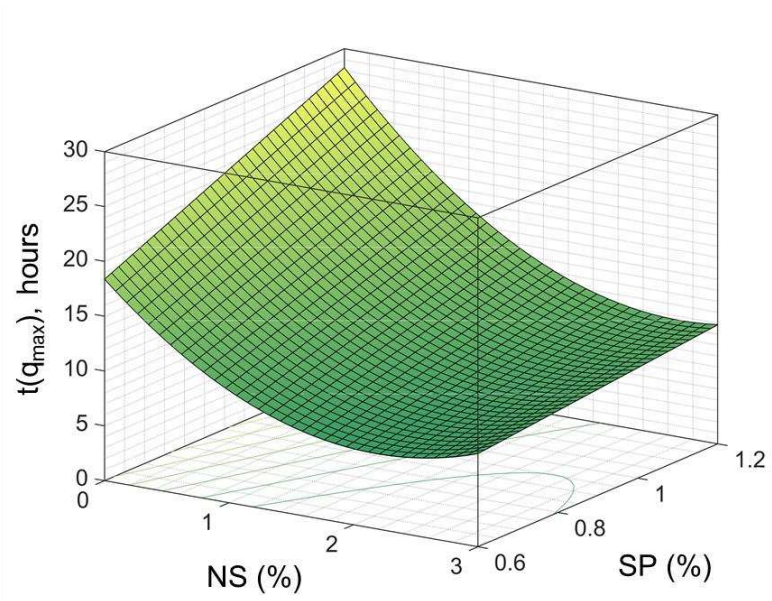

Figure 5. Time to the peak of hydration vs NS and SP dosage, for a GO content of 0.018%.

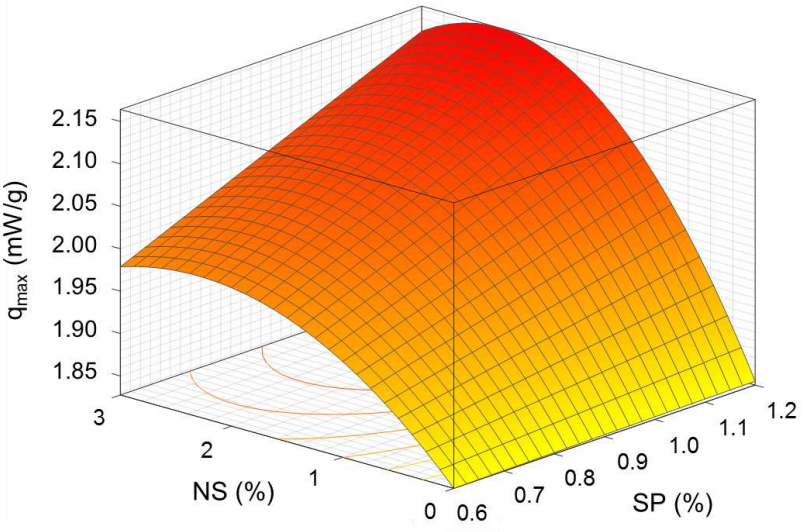

Figure 6. Maximum heat rate vs NS content and SP dosage, for a GO content of 0.018%.

The contour plot in Figure 7 was obtained by plotting equation (4) against NS and GO contents, assuming the SP dosage as 0.6%. It can be seen that incorporating GO increased the peak of hydration, and that its effect on q_{max} was comparable in magnitude to that observed with respect to increasing NS contents. This is consistent with previous studies reporting that the combined addition of NS and GO accelerates cement hydration and improves the cement hydration reactions [32]. Also, the trend followed by q_{max} with respect to the GO content was practically the same for any NS content, and vice versa, suggesting that, when used together, the contribution of both NS and GO is cumulative rather than synergistic. For a constant SP dosage of 0.6%, the addition of GO at 0.03% increased q_{max} by 13.5% on average.

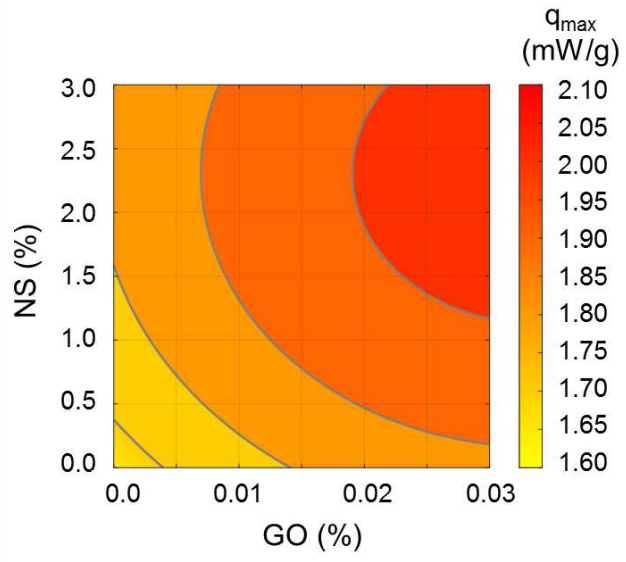

Figure 7. Maximum heat rate vs NS and GO contents for a SP dosage of 0.6%.

However, the optimal GO content was found to vary with the SP dosage, as is clearly observed in Figure 8, where the NS content was assumed at 2.4%. The GO content that maximized q_{max} was 0.03% for an SP dosage of 0.6%, but this optimum decreased for increasing SP dosages, being 0.015% for an SP dosage of 1.2%. For any SP dosage between 0.6% and 1.2%, irrespective of NS content, the addition of GO at the corresponding optimum content increased q_{max} between 11% and 15%.

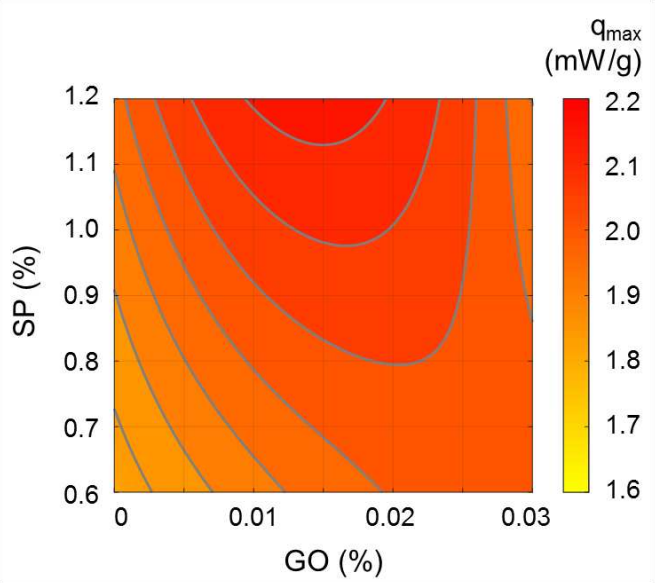

Figure 8. Maximum heat rate vs GO content and SP dosage, for a NS content of 2.5%.

Regarding the parameters $t(q_{min})$ and q_{min}, it was found that they followed very similar trends to those observed for $t(q_{max})$ and q_{max}, respectively. Therefore the conclusions that can be drawn from discussing equations (5) and (6) would be analogous to those already presented in relation to equations (3) and (4).

3.3. Compressive Strength

Average compressive strength values, f_c, and the corresponding standard deviation, $s(f_c)$, at the age of 28 days, both expressed in MPa, are shown in Table 5. Multiple linear regression was used to model the relationship between f_c and the GO, NS contents and SP dosage, expressed in percentage, obtaining the following equation (R-squared=0.81):

$$f_c = 63.9 + 38.1NS - 9.7NS^2 + 762GO + SP(3.5NS - 10.9) + GO\ NS\ (273.3NS - 1187) \quad (7)$$

Table 5. Compressive strength (average and standard deviation) and water sorptivity coefficient at 28 days.

SP (%)	GO (%)	NS (%)	f_c (MPa)	$s(f_c)$ (MPa)	k (cm/s$^{0.5}$)
0.6	0.00	0.0	57.8	3.19	3.567
0.6	0.00	1.0	86.9	4.1	3.774
0.6	0.00	3.0	89.5	3.52	6.538
0.6	0.01	0.0	67.4	6.38	4.144
0.6	0.01	1.0	85.5	1.73	2.863
0.6	0.01	3.0	88.9	3.74	5.649
0.6	0.03	0.0	79.4	4.06	5.361
0.6	0.03	1.0	82.1	0.50	4.054
0.6	0.03	3.0	80.1	4.27	6.994
1.2	0.00	0.0	51.3	1.19	3.586
1.2	0.00	1.0	84.3	2.79	4.325
1.2	0.00	3.0	88.9	3.49	4.276
1.2	0.01	0.0	54.9	2.57	3.644
1.2	0.01	1.0	82.7	8.59	5.008
1.2	0.01	3.0	87.9	0.49	4.131
1.2	0.03	0.0	75.0	1.83	4.791
1.2	0.03	1.0	80.0	1.36	3.875
1.2	0.03	3.0	79.0	4.52	2.722

Figure 9 shows the contour plots defined by equation (7) against NS and GO contents, for the two SP dosages considered. It can be seen that the effect of varying the SP dosage between 0.6% and 1.2% on compressive strength was of minor importance when compared to that of variations in GO or NS contents, and negligible when the NS content is 2% or higher. Therefore, compressive strength was found to be almost insensitive to variations in the SP dosage as long as it falls within the recommended range.

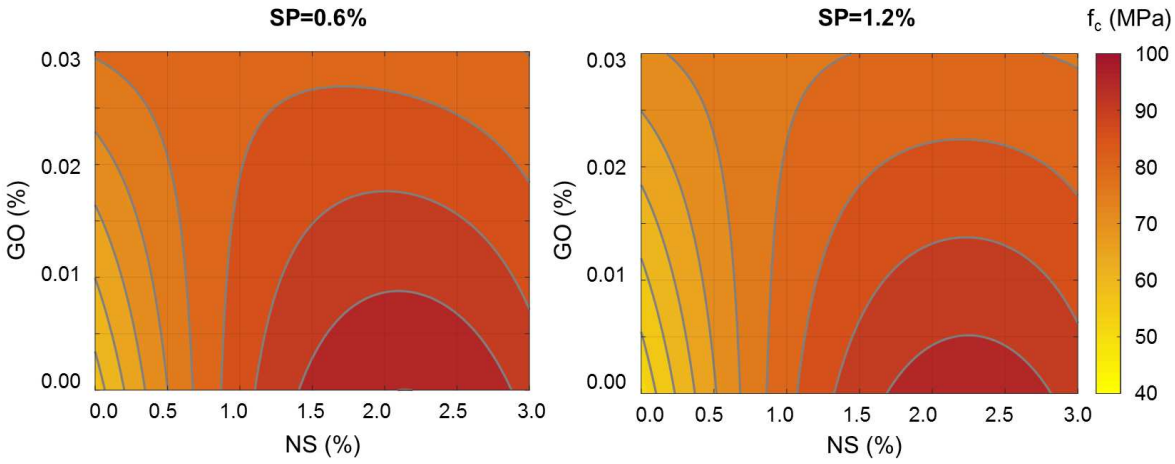

Figure 9. Compressive strength vs NS and GO contents.

The relationship between the GO content and compressive strength was linear, in contrast with the quadratic trend followed by f_c values with respect to NS contents. Also, it was detected that there is a statistically significant interaction between NS and GO, resulting in a modification of the trends observed for f_c with respect to any of the two, depending on the content of the other. The introduction of NS caused f_c values to increase by up to 83%, and there was a clear optimum at 2.2%. This optimal NS content from the point of view of compressive strength was consistent with the optima derived from the workability and calorimetry results (between 2% and 2.4%, respectively), which indicates that NS contents in the region of 2.2% can be considered optimal regarding the properties studied in this paper. However, the effect of NS on f_c values was less important when GO was present at relatively high dosages. Conversely, the effect of GO on f_c was significant but it depended on the NS content. In the absence of NS, the addition of GO at 0.03% increased f_c values by 40.3% to 45.5% (for SP dosages between 0.6% and 1.2% respectively), which is in agreement with compressive strength gains due to GO reported in previous literature [6,24–27,29,33]. Considering the GO content at 0.018% instead, which was identified as the optimum in terms of enhancing cement hydration, its addition to a mix without NS

increased compressive strength by 25.8%. However, in pastes with NS contents of 1% or higher, the addition of GO did not yield significant improvements.

The above discussion of the NS-GO interaction in terms of their combined effect on compressive strength was summarized in Figure 10, where four different cases were compared: pastes with neither GO nor NS, pastes with the optimal amount of NS, pastes with the optimal amount of GO, and pastes with both NS and GO. It was concluded that the addition of either NS or GO was associated with higher f_c values, and that when used in combination they yielded higher f_c values than when only GO was used. However, the highest levels of compressive strength were associated to the cases with only NS.

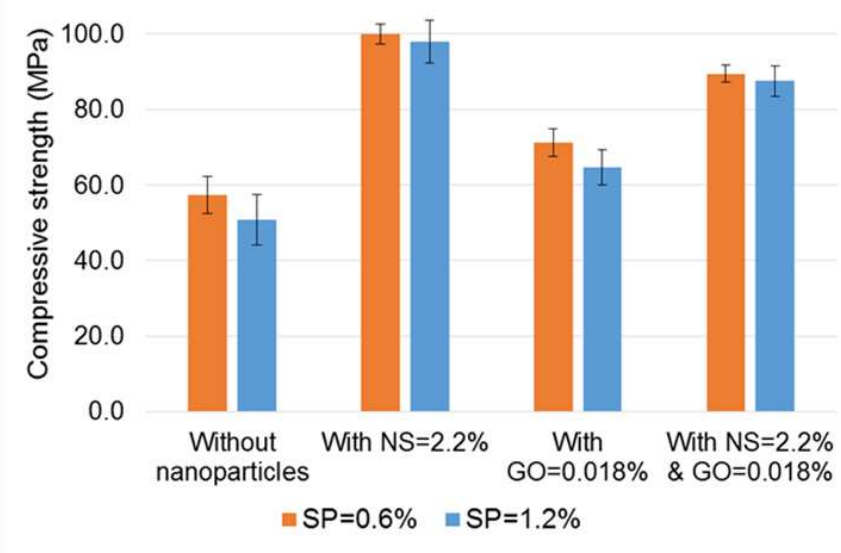

Figure 10. Comparison between different illustrative cases in terms of compressive strength.

3.4. Water Sorptivity

The values of the water sorptivity coefficient, k in cm/s$^{0.5}$, are given in Table 5. The multiple linear regression analysis produced the following equation (R-squared=0.91):

$$k \times 10^3 = 3.76 + GO(158.1SP - 135.8) + GO^2(7776 - 7527SP) + NS(3.38SP - 3.2) + NS^2(1.7 - 1.6SP) - 20.2\ GO\ NS \quad (8)$$

Figure 11 shows the contour plots obtained by plotting equation (8) against NS and GO contents, for the two SP dosages considered in this study. For SP dosage of 0.6%, it was observed that NS contents higher than 1% were associated with higher sorptivity, which was attributed to the difficult dispersion of moderate to high NS contents when the SP dosage was on the lower end of the range of values considered. A similar trend was observed with respect to increasing GO contents beyond 0.015%. However, the incorporation of GO in contents between 0.01% and 0.02% proved beneficial in maintaining low sorptivity. The addition of GO in contents within that range, when the SP dosage was 0.6%, was found to decrease the sorptivity coefficient in percentages between 10% and 17%, for NS contents between 1% and 3%. Therefore, the addition of GO at relatively low dosages proved effective in controlling sorptivity when NS is also present in the mix and the SP dosage is on the lower end.

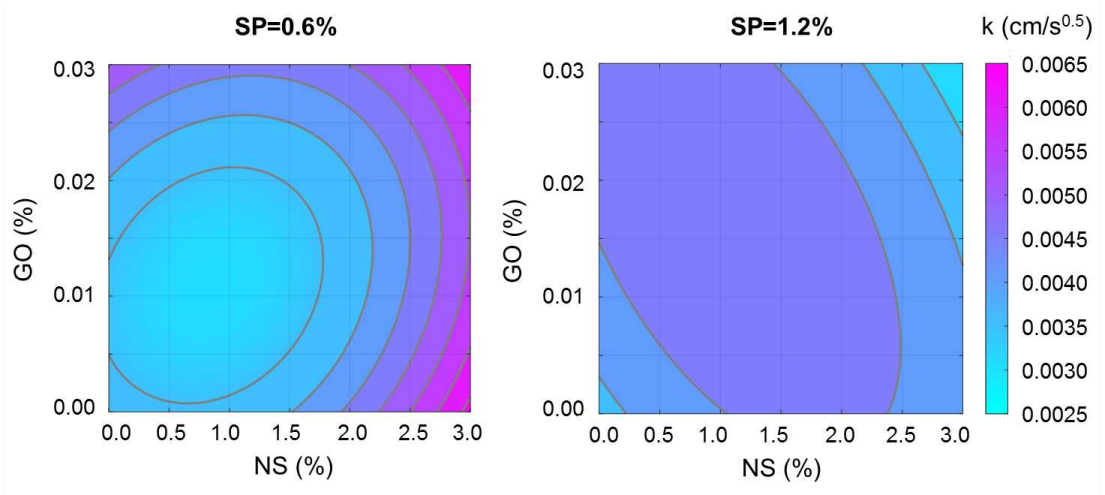

Figure 11. Sorptivity vs NS and GO contents for SP dosages of 0.6% (left) and 1.2% (right).

The comparison of between the two contour plots in Figure 11 confirmed that the relationship between the sorptivity coefficient and the NS and GO contents was significantly sensitive to changes in the SP dosage. When the SP dosage was increased to

1.2%, there was a general reduction of the sorptivity coefficient, and the lowest sorptivity was associated with the combined addition of GO and NS, yielding reductions of up to 22% with respect to the case without any GO or NS. In other words, the combined use of GO and NS led to the highest reductions in the sorptivity coefficient when the SP dosage was on the higher end of its recommended, as the contour plots in Figure 12 show. These contour plots show the sorptivity coefficient as per equation (8) against SP dosage and NS or GO content, assuming a constant GO content of 0.018% or a constant NS content of 2.5% respectively, in line with the optimal contents derived from the analysis of the workability, calorimetry and compressive strength results.

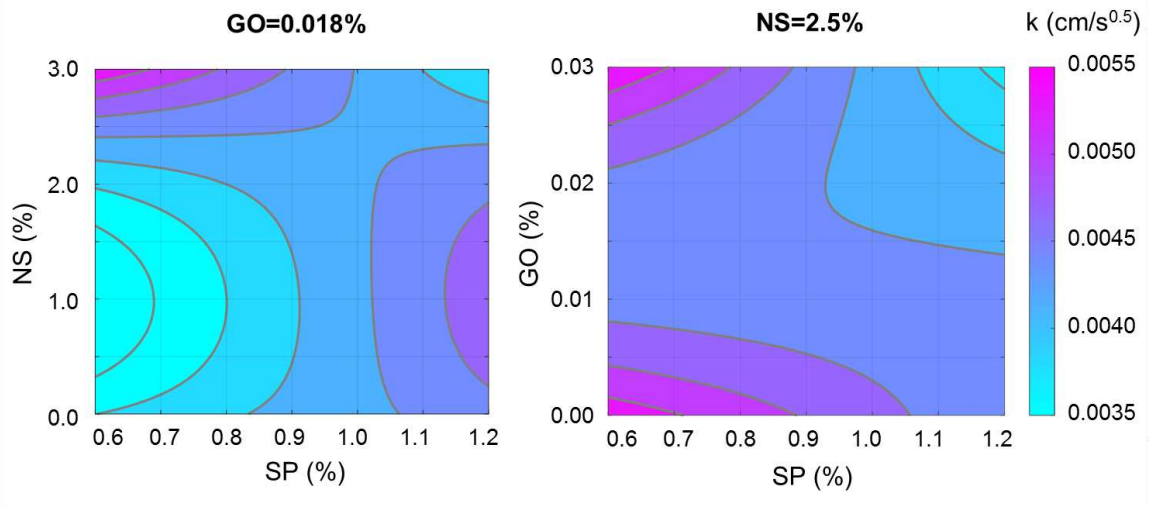

Figure 12. Effect of SP dosage on the sorptivity coefficient when GO content is 0.018 (left) and when NS content is 2.5% (right).

Figure 12(left) shows that the relationship between the sorptivity coefficient and the SP dosage was strongly dependent on the NS content, and the effect that increasing the SP dosage had on sorptivity gained significance for increasing NS contents. Increasing the SP dosage from 0.6% to 1.2% was found to cause reductions in the sorptivity coefficient of up to 35% when the NS content was 3%. This was attributed to the enhanced dispersion of the

NS particles resulting from higher SP dosages, which gained significance when the NS contents considered were high. This was also true in relation to GO particles, as can be seen in Figure 12(right), where increasing SP dosages were associated to lower sorptivity values when high GO contents are considered together with an NS content of 2.2%.

4. CONCLUSIONS

Portland cement pastes incorporating GO and NS in dosages of up to 0.03% and 3% respectively were tested to evaluate their effects when they are used in combination, and to what extent their effect was influenced by variations in the SP dosage between 0.6%and 1.2%. The properties analyzed were: flowability, heat of hydration, compressive strength and water sorptivity at 28 days. The following conclusions were obtained:

- For GO and NS contents below 0.02% and 1% respectively, it was concluded that SP dosages on the lower end of their recommended range were generally sufficient to achieve good levels of flowability. The addition of GO and NS at higher rates proved detrimental to the performance of fresh cement pastes and had to be counterbalanced by increasing the SP dosage in order to maintain the flowability. However, when GO and NS were used in combination, NS dominated the reduction in flowability and the increasing SP dosage requirements.
- Both NS and GO were observed to accelerate cement hydration and to increase the intensity of the peak of hydration. The accelerating effect of GO was found to be most advantageous when added in combination with NS. The efficiency of both GO and NS in enhancing cement hydration was found to be significantly improved by increasing SP dosages, which was attributed to the beneficial effect that SP has on the dispersion of these nanoparticles in fresh cement-based systems.

- Optimal GO and NS contents were found to be in the region of 0.018% and 2.2% respectively, and were consistent for all the properties under consideration (workability, cement hydration, compressive strength, and water sorptivity).
- Compressive strength at 28 days was confirmed to significantly improve with the addition of either GO, NS, or both combined.
- The addition of GO in combination with NS proved effective in minimizing the water sorptivity. Reductions in the water sorptivity coefficient of up to 22% were obtained for GO and NS contents of 0.018% and 2.2% respectively. Increasing the SP dosage proved beneficial in further reducing the water sorptivity coefficient, and reductions of up to 35% were obtained by increasing the SP dosage from 0.6% to 1.2% when the GO and NS contents were 0.03% and 3% respectively.

Acknowledgments: The authors wish to acknowledge the support received from the following companies, which kindly provided the materials used in this research: AkzoNobel, BASF, and Versarien 2D Tech.

Funding: This research did not receive any specific grant from funding agencies in the public, commercial, or not-for-profit sectors.

REFERENCES

[1] Kawashima S, Hou P, Corr DJ, Shah SP. Modification of cement-based materials with nanoparticles. Cement Concrete Comp 2013;36:8–15. doi:10.1016/j.cemconcomp.2012.06.012.

[2] Pacheco-Torgal F, Jalali S. Nanotechnology: Advantages and drawbacks in the field of construction and building materials. Constr Build Mater 2011;25:582–90. doi:10.1016/j.conbuildmat.2010.07.009.

[3] Chuah S, Pan Z, Sanjayan JG, Wang CM, Duan WH. Nano reinforced cement and concrete composites and new perspective from graphene oxide. Constr Build Mater 2014;73:113–24. doi:10.1016/j.conbuildmat.2014.09.040.

[4] Sanchez F, Sobolev K. Nanotechnology in concrete – A review. Constr Build Mater 2010;24:2060–71.

[5] Senff L, Hotza D, Lucas S, Ferreira VM, Labrincha JA. Effect of nano-SiO2 and nano-TiO2 addition on the rheological behavior and the hardened properties of cement mortars. Mater Sci Eng A-Struct 2012;532:354–61. doi:10.1016/j.msea.2011.10.102.

[6] Pan Z, He L, Qiu L, Korayem AH, Li G, Zhu JW, et al. Mechanical properties and microstructure of a graphene oxide–cement composite. Cement Concrete Comp 2015;58:140–7. doi:10.1016/j.cemconcomp.2015.02.001.

[7] Alkhateb H, Al-Ostaz A, Cheng AH-D, Li X. Materials Genome for Graphene-Cement Nanocomposites. J Nanomech Micromech 2013;3:67–77. doi:10.1061/(ASCE)NM.2153-5477.0000055.

[8] Jalal M, Pouladkhan A, Harandi OF, Jafari D. Comparative study on effects of Class F fly ash, nano silica and silica fume on properties of high performance self compacting concrete. Constr Build Mater 2015;94:90–104. doi:10.1016/j.conbuildmat.2015.07.001.

[9] García-Taengua E, Sonebi M, Hossain KMA, Lachemi M, Khatib J. Effects of the addition of nanosilica on the rheology, hydration and development of the compressive strength of cement mortars. Compos Part B-Eng 2015;81:120–9. doi:10.1016/j.compositesb.2015.07.009.

[10] Lim S, Mondal P. Effects of incorporating nanosilica on carbonation of cement paste. J Mater Sci 2015;50:3531–40. doi:10.1007/s10853-015-8910-7.

[11] Sonebi M, García-Taengua E, Hossain KMA, Khatib J, Lachemi M. Effect of nanosilica addition on the fresh properties and shrinkage of mortars with fly ash and superplasticizer. Constr Build Mater 2015;84:269–76. doi:10.1016/j.conbuildmat.2015.02.064.

[12] Senff L, Labrincha JA, Ferreira VM, Hotza D, Repette WL. Effect of nano-silica on rheology and fresh properties of cement pastes and mortars. Constr Build Mater 2009;23:2487–91. doi:10.1016/j.conbuildmat.2009.02.005.

[13] Sobolev K, Flores I, Torres-Martinez LM, Valdez PL, Zarazua E, Cuellar EL. Engineering of SiO2 Nanoparticles for Optimal Performance in Nano Cement-Based Materials. Nanotechnology in Construction 3, Berlin, Heidelberg: Springer Berlin Heidelberg; 2009, p. 139–48. doi:10.1007/978-3-642-00980-8_18.

[14] Korayem AH, Tourani N, Zakertabrizi M, Sabziparvar AM, Duan WH. A review of dispersion of nanoparticles in cementitious matrices: Nanoparticle geometry perspective. Constr Build Mater 2017;153:346–57. doi:10.1016/j.conbuildmat.2017.06.164.

[15] Said AM, Zeidan MS, Bassuoni MT, Tian Y. Properties of concrete incorporating nano-silica. Constr Build Mater 2012;36:838–44. doi:10.1016/j.conbuildmat.2012.06.044.

[16] Du H, Du S, Liu X. Durability performances of concrete with nano-silica. Constr Build Mater 2014;73:705–12. doi:10.1016/j.conbuildmat.2014.10.014.

[17] Abd.El.Aleem S, Heikal M, Morsi WM. Hydration characteristic, thermal expansion and microstructure of cement containing nano-silica. Constr Build Mater 2014;59:151–60. doi:10.1016/j.conbuildmat.2014.02.039.

[18] Jo B-W, Kim C-H, Tae G, Park J-B. Characteristics of cement mortar with nano-SiO2 particles. Constr Build Mater 2007;21:1351–5. doi:10.1016/j.conbuildmat.2005.12.020.

[19] Nazari A, Riahi S. The effects of SiO2 nanoparticles on physical and mechanical properties of high strength compacting concrete. Compos Part B-Eng 2011;42(3):570-578. doi:10.1016/j.compositesb.2010.09.025

[20] Janković K, Stanković S, Bojović D, Stojanović M, Antić L. The influence of nano-silica and barite aggregate on properties of ultra high performance concrete. Constr Build Mater 2016;126:147–56. doi:10.1016/j.conbuildmat.2016.09.026.

[21] Park S, Ruoff RS. Chemical methods for the production of graphenes. Nat Nanotechnol 2009;4:217–24. doi:10.1038/nnano.2009.58.

[22] Peng L, Xu Z, Liu Z, Wei Y, Sun H, Li Z, et al. An iron-based green approach to 1-h production of single-layer graphene oxide. Nat Commun 2015;6:1–9. doi:10.1038/ncomms6716.

[23] Lu Z, Li X, Hanif A, Chen B, Parthasarathy P, Yu J, et al. Early-age interaction mechanism between the graphene oxide and cement hydrates. Constr Build Mater 2017;152:232–9. doi:10.1016/j.conbuildmat.2017.06.176.

[24] Gong K, Asce SM, Pan Z, Korayem AH, Ph D, Qiu L, et al. Reinforcing Effects of Graphene Oxide on Portland Cement Paste J Mater Civil Eng 2015;27:1–6. doi:10.1061/(ASCE)MT.1943-5533.0001125.

[25] Wang Q, Wang J, Lu C, Liu B, Zhang K, Li C. Influence of graphene oxide additions on the microstructure and mechanical strength of cement. New Carbon Mater 2015;30:349–56. doi:10.1016/S1872-5805(15)60194-9.

[26] Li X, Liu YM, Li WG, Li CY, Sanjayan JG, Duan WH, et al. Effects of graphene oxide agglomerates on workability, hydration, microstructure and compressive strength of cement paste. Constr Build Mater 2017;145:402–10. doi:10.1016/j.conbuildmat.2017.04.058.

[27] Li X, Lu Z, Chuah S, Li W, Liu Y, Duan WH, et al. Effects of graphene oxide aggregates on hydration degree, sorptivity, and tensile splitting strength of cement paste. Compos Part A-Appl S 2017;100:1–8. doi:10.1016/j.compositesa.2017.05.002.

[28] Mokhtar MM, Abo-El-Enein SA, Hassaan MY, Morsy MS, Khalil MH. Mechanical performance, pore structure and micro-structural characteristics of graphene oxide nano platelets reinforced cement. Constr Build Mater 2017;138:333–9. doi:10.1016/j.conbuildmat.2017.02.021.

[29] Mohammed A, Sanjayan JG, Duan WH, Nazari A. Incorporating graphene oxide in cement composites: A study of transport properties. Constr Build Mater 2015;84:341–7. doi:10.1016/j.conbuildmat.2015.01.083.

[30] Shang Y, Zhang D, Yang C, Liu Y, Liu Y. Effect of graphene oxide on the rheological properties of cement pastes. Constr Build Mater 2015;96:20–8. doi:10.1016/j.conbuildmat.2015.07.181.

[31] Oltulu M, Şahin R. Single and combined effects of nano-SiO2, nano-Al2O3 and nano-Fe2O3 powders on compressive strength and capillary permeability of cement mortar containing silica fume. Mater Sci Eng A-Struct 2011. doi:10.1016/j.msea.2011.05.054.

[32] Zhao, L., Xinli, G., Yuanyuan, L., Chuang G., Liping G., Xin S., Jiaping, L. Synergistic effects of silica nanoparticles/polycarboxylate superplasticizer modified graphene oxide on mechanical behavior and hydration process of cement composites. RSC Advances 2017; 7(27): 16688–702. doi:10.1039/C7RA01716B.

[33] Liu, H., Yongjin Y., Huimin L., Jianzhou J., Shuoqiong L. Hybrid effects of nano-silica and graphene oxide on mechanical properties and hydration products of oil well cement. Constr Build Mater 2018; 191(Dec):311-319. doi:10.1016/j.conbuildmat.2018.10.029.

[34] European Committee for Standardization. EN 445:2007 Grout for prestressing tendons. Test methods 1997.

[35] European Committee for Standardization. EN 196-1:2016 Methods of testing cement. Determination of Strength 2016.

[36] European Committee for Standardization. EN 12390-3:2009 Testing hardened concrete - Part 3: Compressive strength of test specimens 2009.

[37] ASTM C1585-13. Standard Test Method for Measurement of Rate of Absorption of Water by Hydraulic Cement Concretes. ASTM International 2013;41:1–6.

[38] Jolicoeur C, Simard M-A. Chemical admixture-cement interactions: Phenomenology and physico-chemical concepts. Cement Concrete Comp 1998;20:87–101. doi:10.1016/S0958-9465(97)00062-0.